

## Measurement of tagged-particle diffusion using delayed two-photon absorption

A. Streater, G. Kintz, and J. Cooper

*Joint Institute for Laboratory Astrophysics, University of Colorado and National Bureau of Standards,  
Boulder, Colorado 80309-0440*

A. Santos

*Departamento de Física Teoría, Facultad de Física, Apartado Correos 1065, Sector Sur,  
Universidad de Sevilla, E-41080 Sevilla, Spain*

K. Burnett

*Department of Physics, Blackett Laboratory, Imperial College of Science and Technology,  
University of London, London SW72BZ, England, United Kingdom*

J. W. Dufty

*Department of Physics, University of Florida, Gainesville, Florida 32611*

(Received 30 December 1985)

A simple experiment on tagged-particle diffusion in a dilute gas has been performed and analyzed. Two lasers were used to prepare and probe a pencil of excited  $^3P_1$  calcium atoms in a background of argon atoms. It was possible to observe the evolution of the "tagged" particles on a time scale extending from free streaming to hydrodynamic (diffusion) behavior. Although this first experiment is only exploratory, a simple analysis of the data indicates the usefulness of the technique for future studies.

The trial experiment discussed below arose mainly because we were trying to find experimental methods for studying Boltzmann gases, far from equilibrium, on space and time scales extending beyond the hydrodynamical regime. A Boltzmann gas is of interest because it is possible to make detailed microscopic calculations of the non-equilibrium state, and of the transport properties associated with these states. Three of us were involved in measurements of time-dependent radiative transport that employ direct observation of evolving atomic state populations and it appeared that the same technique would be applicable here.<sup>1</sup> The basic idea is to produce a set of tagged particles in a gas using laser excitation and map out its evolution in space and time directly. Because signal detection by this method is possible at very low densities, the space and time scales relative to the mean free path and time are different from those of current experimental methods. The experiment we describe here is an equilibrium experiment. The experiment, along with its analysis, is rather crude, but they do give enough of a basis to justify more precise experiments to be planned and executed. Some interesting extensions along with other ramifications are also indicated briefly.

The experiment is sketched in Fig. 1. A stainless-steel cell was first evacuated and then charged with calcium metal in an argon atmosphere. The cell was heated to produce a vapor of calcium. In the experiments the cell temperature was 585°C producing a number density of  $\sim 10^{13}$  cm<sup>-3</sup> for the calcium. The argon density was always much larger than this,  $\sim (10^{15}-10^{17})$  cm<sup>-3</sup>. Two pulsed dye lasers were used to produce and probe calcium  $4s4p^3P_1$  metastables. The first laser pumped the

( $^1S_0 \rightarrow ^3P_1$  "forbidden") transition at  $\lambda = 657.3$  nm. This produced a pencil of excitation along the center of the cell approximately 300  $\mu$ m in diameter. The second laser was displaced spatially from the excitation region and delayed in time. This delay was achieved by timing the Q-switched pulses of the two Nd-YAG pump lasers. The second laser pumped atoms from the  $4s4p^3P_1$  to the  $4s5s^3S$  which then decay rapidly and emit radiation around 612 nm. This spontaneous emission was detected using a photomultiplier and recorded using a gated integrator linked to a Cromemco minicomputer. This 612-nm fluorescence is proportional to the density of the  $4s4p^3P_1$  atoms at the time and spatial position of the

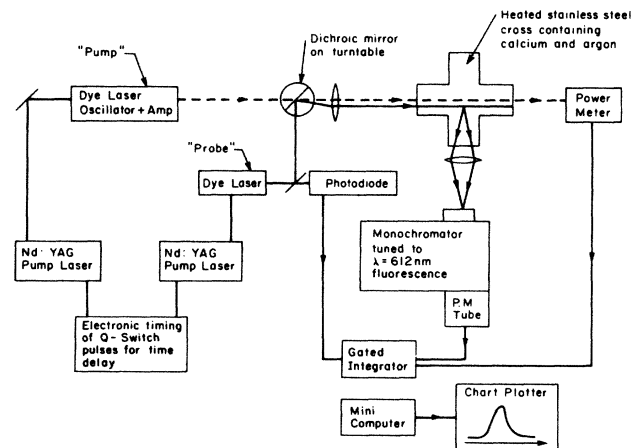


FIG. 1. Schematic diagram of the experiment.

probe pulse. The profile of the excitation of  $^3P_1$  atoms was recorded at several delays by scanning the second laser beam across the first to map out a spatial distribution of the "labeled" Ca atoms at fixed time delay.

The experiment essentially measures the joint probability density  $G(\mathbf{r}, t; \mathbf{r}_0, 0)$  for the excited Ca\* atoms. This quantity gives the probability for detecting an excited Ca\* atom at  $(\mathbf{r}, t)$ , having created it at  $(\mathbf{r}_0, t=0)$ . Due to finite excitation and detection resolution the quantity observed is the spatial convolution of  $G(\mathbf{r}, t; \mathbf{r}_0, 0)$  with two characteristic functions,

$$S(z, t) = \int d\mathbf{r} d\mathbf{r}_0 I_z(\mathbf{r}) I_0(\mathbf{r}_0) G(\mathbf{r}, t; \mathbf{r}_0, 0). \quad (1)$$

Here  $I_z(\mathbf{r})$  defines the long pencil-like probe beam profile, orthogonal to the  $z$  axis and centered about the point  $z$ . The probe beam profile can be measured by scanning a pinhole. The cross section of the initial excitation  $I_0(\mathbf{r})$  can be thought of as approximately a circle of diameter  $d \sim 300 \mu\text{m}$ , whereas the effective length of the pencil is  $\geq 1$  cm. In general,  $I_0(\mathbf{r}_0)$  can be determined experimentally to within a few percent, and it may be convenient to vary  $d$  for some purposes. The pumping times for the metastables is about 10 ns while their lifetime is about 1 ms due to fine-structure changing collisions.<sup>2</sup> This defines the time scales for which Eq. (1) can be studied. The spatial resolution is limited by  $d$ , which could be made as small as  $\sim 10 \mu\text{m}$  with a spatially filtered pump laser. There are no limitations on the maximum values of  $z$ . These space and time scales are significantly different from those of neutron scattering or Brillouin light scattering experiments typically used to measure dynamic fluctuations in gases. In particular, the larger space and time scales open the possibility for study of nonequilibrium phenomena, as discussed below, that are difficult to observe with neutrons or light scattering.

The Green's function  $G(\mathbf{r}, t; \mathbf{r}_0, 0)$  is a Gaussian function of  $|\mathbf{r} - \mathbf{r}_0|$  at both asymptotically short times (free streaming) and long times (diffusion). The primary characteristic feature of  $S(z, t)$  is therefore its width (at half maximum) as a function of time,  $\xi(t)$ , which describes the transition between kinetic and hydrodynamic stages for the transport of the Ca\* atoms. Table I shows the experimental conditions of pressure and time sampled and the associated widths  $\xi(t)$  observed.

A simple model that incorporates both short and long time limits is the Gaussian model,<sup>3</sup> for which  $G(\mathbf{r}, t; \mathbf{r}_0, 0)$  obeys the usual diffusion equation but with a time-dependent diffusion coefficient

$$D(t) \equiv \frac{1}{3} \int_0^t d\tau \langle \mathbf{v} \cdot \mathbf{v}(\tau) \rangle. \quad (2)$$

In this model, the width of  $G(\mathbf{r}, t; \mathbf{r}_0, 0)$  is proportional to  $[\alpha(t)]^{1/2}$ , where

$$\alpha(t) \equiv \int_0^t d\tau D(\tau). \quad (3)$$

The short-time (free streaming) behavior ( $t/t_0 \ll 1$ ) is given by  $\alpha(t) \rightarrow \frac{1}{6} \langle v^2 \rangle t^2$ ; thus this model describes the short-time behavior of  $G(\mathbf{r}, t; \mathbf{r}_0, 0)$  exactly. In this limit the particles move freely and the distribution function obeys the evolution rule

TABLE I. Experimental widths  $\xi(t)$  of  $S(z, t)$ .

$p$ (torr)	$t$ (ns)	$\xi$ ( $\mu\text{m}$ )	$t/t_0$	$\alpha/D(\infty)t_0$
1	20	511 $\pm$ 5	0.048	0.001
	50	523 $\pm$ 9	0.119	0.037 $\pm$ 0.042
	100	520 $\pm$ 9	0.238	0.028 $\pm$ 0.042
	200	526 $\pm$ 23	0.476	0.046 $\pm$ 0.085
	350	607 $\pm$ 7	0.833	0.311 $\pm$ 0.039
4	40	480 $\pm$ 8	0.381	0.072
	100	480 $\pm$ 12	0.952	0.07 $\pm$ 0.89
	200	513 $\pm$ 8	1.905	1.58 $\pm$ 0.73
	350	531 $\pm$ 3	3.333	2.45 $\pm$ 0.50
10	20	465 $\pm$ 5	0.476	0.113
	100	470 $\pm$ 10	2.381	1.5 $\pm$ 4.1
	300	486 $\pm$ 10	7.143	5.9 $\pm$ 4.1
40	100	493 $\pm$ 7	9.524	
	350	500 $\pm$ 7	33.33	

$$f(\underline{\mathbf{r}}, \underline{\mathbf{v}}, t) = f(\underline{\mathbf{r}} - \underline{\mathbf{v}}t, \underline{\mathbf{v}}, 0),$$

and the behavior of the excited-state number density  $n(\underline{\mathbf{r}}, t) = \int d\underline{\mathbf{v}} f(\underline{\mathbf{r}}; \underline{\mathbf{v}}; t)$  given by this rule agrees exactly with the Gaussian model.

In the long-time (diffusion) limit,  $\alpha(t) \rightarrow D(\infty)t$ . Therefore, the Gaussian model is exact for short times, and provides the diffusion limit for long times. It is also a good interpolation between these two limits.<sup>4,5</sup> The width of  $S(z, t)$  depends, of course, on the form of  $G$ , the probe beam profile and the form of the initial distribution. To be precise, it is a convolution of these functions, as shown in Eq. (1). We approximate the spatial distribution for the pump and probe beams by Gaussian functions. After the convolution is taken over the initial distribution and probe beam profile, the relationship between the observed width  $\xi(t)$  and  $\alpha(t)$  is simply

$$\xi^2(t) = \xi^2(0) + 16 \ln 2 [\alpha(t)], \quad (4)$$

where  $\xi(0)$  is the initial excitation width plus the probe beam width added in quadrature. Thus for small times the width is proportional to

$$\left[ \frac{3\xi^2(0)}{8 \ln 2} + v^2 t^2 \right]^{1/2},$$

and for long times is proportional to  $\sqrt{Dt}$  [for  $Dt \gg \xi(0)$ ].

We have fitted the initial width  $\xi(0)$  at each pressure (except at  $p = 40$  torr) by assuming that, in each case, the experimental shortest-time datum lies on the free streaming region. This allows us to obtain  $\alpha(t)$  at the remaining times. It is convenient to introduce an effective "mean free time"  $t_0$  by the definition  $D(\infty) \equiv \frac{1}{3} \langle v^2 \rangle t_0$ . For a low density gas,  $t_0$  is inversely proportional to the pressure:  $t_0 \equiv (mk_B T/6)^{1/2}/(p\sigma)$ , where  $\sigma$  is an effective cross section of the Ca\*-Ar scattering. An estimate of  $\sigma$  is obtained by assuming that  $\alpha(t)$  is in the diffusion limit

for the highest pressure ( $p = 40$  torr) data and for  $p = 10$  torr,  $t = 300$  ns. The result is  $\sigma = (20 \pm 14) \text{ \AA}^2$ , which is consistent with calculations based on the Coulomb approximation.<sup>6</sup> (Note, however, a more precise determination is mentioned below.) The third and fourth columns of Table I show the experimental times relative to  $t_0$  and the reduced quantity  $\alpha(t)/D(\infty)t_0$ . Clearly, both short and long times have been studied relative to the mean free time, although only sparsely. Figure 2 shows the experimental values of  $\alpha(t)/D(\infty)t_0$  as a function of  $t/t_0$ . Also shown is the result for a simple model of the velocity autocorrelation function with exponential decay (such a model is well known to be a good approximation at low density<sup>7</sup>). The corresponding form for  $\alpha(t)$  is then

$$\alpha(t) = \frac{1}{3} \langle v^2 \rangle t_0^2 [e^{-t/t_0} + (t/t_0) - 1]. \quad (5)$$

This simple model is in reasonable agreement with the experimental points. A better fit could be obtained if one uses Eq. (5) to adjust  $\xi(0)$  (at each pressure) and  $\alpha$ . By doing so, the value  $\sigma = (18.3 \pm 1.7) \text{ \AA}^2$  is obtained. We have also checked that the results are quite insensitive to the assumed shape of the pump and probe beams.

A repeat of this type of equilibrium experiment with higher precision is planned, to sample in detail the complete transition range  $0 < (t/t_0) \leq 100$ . The measurements presented here were crude only because the time delays were limited by the electronics to about 350 ns. Experimental uncertainties could be considerably reduced by using longer time delays. One obvious advantage of this technique is the ability to determine diffusion coefficients of atoms and molecules in metastable states, for which conventional methods are inapplicable. Furthermore, the only other method for studying the transition region for tagged particles (inelastic neutron scattering) is limited to liquids or dense gases. The present method has the capacity to study this region at low densities where the theoretical developments are generally assumed to be most complete. In this sense it is an interesting complement to neutron and light scattering studies of fluids.

The experimental study of transport<sup>8</sup> and fluctuations<sup>9</sup> in nonequilibrium systems is even more limited. Nonequilibrium states involve changes in the hydrodynamic variables over space and time scales that are large compared to those sampled by light or neutron scattering. The deviations from equilibrium are measured by a uniformity parameter  $\mu = l/L$  where  $l$  is the mean free path and  $L$  is the distance over which the relative changes in the hydrodynamic variables is of order 1. Current experi-

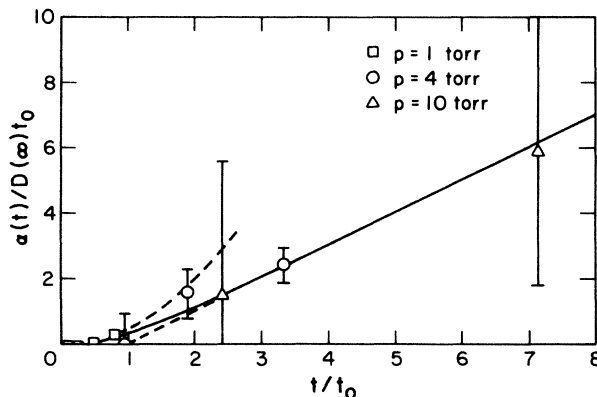


FIG. 2. Plot of  $\alpha(t)/D(\infty)t_0$  vs  $t/t_0$  from the experimental data. The solid line corresponds to the model defined by Eq. (5). The asymptotic short-time and long-time behaviors are also shown (dashed lines).

mental methods are limited by a maximum value of  $l$  (minimum density) because of signal loss. Consequently, to increase  $\mu$  large gradients in the hydrodynamic variables must be produced; convective instabilities and other problems have restricted the nonequilibrium states to  $10^{-2} \lesssim \mu < 10^{-1}$ . The method described here has the potential to improve on these limitations by increasing the mean free path  $l$  instead of decreasing  $L$ . Since the fluorescence signals are easily detected at low pressures,  $\mu$  can be increased simply by lowering the pressure. For example, at  $10^{-1}$  torr the mean free path can be of the order of  $10^{-1}$  cm. Thus the microscopic scales can be amplified to the macroscopic levels characterizing the nonequilibrium states available. For similar reasons the singular transitions from a collisional gas to a Knudsen gas can be studied for finite geometries, by changing the Knudsen number as a function of pressure. We are not aware of any alternative to spectroscopic techniques for investigation of such low densities. A class of nonequilibrium experiments along these lines is being explored.

A. Streater was supported by Lawrence Livermore National Laboratory, G. Kintz and J. Cooper by the U. S. Air Force Office of Scientific Research under Grant No. AFOSR 840027, A. Santos by the Alianza Espana-Florida, and K. Burnett and J. W. Dufty in part by the National Science Foundation under Grant No. CHE-84-11932.

<sup>1</sup>W. A. Molander, M. Belsley, A. Streater, and K. Burnett, *Phys. Rev. A* **29**, 1548 (1984).

<sup>2</sup>G. Kintz and J. Cooper (unpublished).

<sup>3</sup>J. P. Hansen and I. R. McDonald, *Theory of Simple Liquids* (Academic, New York, 1976).

<sup>4</sup>R. Desai, *J. Chem. Phys.* **44**, 77 (1966).

<sup>5</sup>L. Groome, J. Dufty, and M. Lindemfeld, *Phys. Rev. A* **19**, 304 (1979).

<sup>6</sup>G. K. Oertel and L. P. Shomo, *Astrophys. J. Suppl.* **16**, 175

(1968).

<sup>7</sup>J. P. Boon and S. Yip, *Molecular Hydrodynamics* (McGraw-Hill, New York, 1980).

<sup>8</sup>F. Baas, P. Oudeman, H. Knapp, and J. Beenaker, *Physica* **89**, A73 (1977).

<sup>9</sup>D. Beysen, Y. Garrabos, and G. Zalczer, *Phys. Rev. Lett.* **45**, 403 (1980); H. Kiefte, M. Clouter, and R. Penny, *Phys. Rev. B* **30**, 4017 (1984).